The nonlinear dynamics of stability in modular networks

Paul Heyden

Research advisor: David A. Egolf

Department of Physics
Georgetown University

May 21, 2021

Submitted in fulfillment of the Senior Thesis requirement
in the Department of Physics, Georgetown University,
Washington, DC, May 2021

Abstract

A network is a group of nodes that are connected to each other. Networks are an important area of study because of their wide range of applications as well as their relevance to modern day life. Transportation and shipping routes, ecological populations of animals, and telecommunications systems are just a few examples. In this thesis, we investigate whether networks are stable based on key features such as modularity (how grouped a network is) and node-to-node population sharing. We find that node-to-node sharing can stabilize an unstable system, and, similarly, sharing can make a stable system unstable. We analytically calculate why this happens, developing a theory of an "effective" parameter μ which decreases as sharing increases. We also observe that higher modularity gives a different pattern of stability (a decrease in stability, followed by an increase and a second decrease) as sharing increases. Next, we observe critical values of sharing (roughly where 20% of the population exchanges between nodes) which make systems susceptible to perturbations that spread throughout the whole system (similarly to a virus spreading globally). Finally, we calculate that with sharing of over 65%, the nodes all synchronize and their values become the same, meaning we can think of the system as a single node which evolves in time.

Contents

Chapter 1

Introduction

Networks consist of a set of objects (people, computers, ecosystems, airports, etc.) called nodes that either communicate with each other, exchanging information or things (populations, diseases, planes, money, etc.), or are related in some way. In sparse networks, such as those discussed in this thesis, each node is typically connected only to a small number of other nodes. Networks are an important area of study because of their wide range of applications as well as their relevance to modern day life. Transportation and shipping routes, electric grids, and telecommunications systems are just a few examples. A network can even be a group of shared agreements or negotiations. Ants communicating about where sugar is found is a network. We can also think of YouTube as a network of related videos, channels, and profiles, each with a population of views or subscribers. Furthermore, democracy can be a network, with groups of people each sharing views and

coming to agreements.

The networks we make use of in daily life, including electrical grids, transportation networks, and the internet, require stability to function. Stability in networks is essential to quality of life. Networked systems – such as populations, ecosystems, financial markets, or air traffic – are susceptible to perturbations that spread, causing failure to different degrees [1]. How vulnerable the system is depends on the system's network structure [2]. Researchers in previous decades found that network size and average number of connections per node are correlated with stability [3, 4]. Researchers have also posited that network stability should correlate with modularity, which is a measure of how connected nodes are internally in their group [4]. How modularity affects network stability is one the main themes I have been studying.

In this thesis, I further the work of Ben Stein-Lubrano and Dr. David Egolf [5]. They studied a computational model of networks of nodes, where each node has a generalized population and has connections to other nodes. The networks we study here are modular, meaning nodes within a group are more likely to be connected to each other than to those outside of the group. This reflects how populations of nodes in the network, such as people on Facebook, transfer more information to nearby nodes than to those further away (with the Facebook example, a distance of one would be a friend, a distance of two would mean a friend of a friend, and so on).

In our model, the nodes share population based on nodes to which they are connected. Using the mathematical tools of nonlinear dynamics, we study the evolution of perturbations in these networks. Perturbations refer to small (in our case, infinitesimal) changes to the populations of one or more nodes. Using Lyapunov exponents and vectors (see methods for a description), we analyze how a perturbed system evolves compared to a corresponding unperturbed system. If the difference between the two systems grows exponentially on average for any possible perturbation, the system is chaotic and thus unstable. Nonlinear dynamics allow us not only to measure whether a network is stable or not but also to characterize the extent of the spread of the perturbation so that we can try to understand when the modularity of a system leads to only localized instability rather than global instability. The nonlinear dynamical tools will be explained in the background and methods sections below.

Ben Stein-Lubrano designed a set of code which generates networks, and he also designed a simulation in which each node's population evolves and shares population with connected nodes. Building on Ben's work, I have expanded his original codes and added the calculation of several new quantities to measure various properties of how perturbation evolve and spread.

Chapter 2

Background

2.1 Work in the last century

Scientists' understanding of how a network's size and structure affects its stability has changed over time, and much research has been done on this topic. In the mid-1950's, MacArthur argued that if a network has more connections for species to interact, then one connection's failure would be less problematic [6]. Similarly, Elton warned that as the complexity of ecosystems is reduced, those ecosystems would be less stable [7]. This view was supported by field studies which showed that as humans disrupt natural environments, the environments would be more susceptible to extinction. Thus, the early view in the field was that complexity is proportional to stability. For example, an environmental textbook [8] in the 1970's claimed that "the accumulation of biological diversity... promotes population sta-

bility." However, some field studies gave contradictory results.

Further, several studies in the 1970's found more varied relationships between stability and network size, as well as degree of connectivity and stability. For example, Gardner and Ashby performed simple numerical studies on the stability of networks with different numbers of nodes and different degrees of connectivity between nodes [3]. They found that systems with higher degrees of connectivity were likely to be less stable for all network sizes they tested. Also, as the size of their networks grew, the system became less stable.

May built on this work with analytical calculations [4]. In addition to connectivity and network size, he included interaction strength as a parameter, where interaction strength denotes the percentage of population shared between nodes. He found that increasing interaction strength also decreased the stability of the network. In addition, he introduced the idea that a larger system can be made more stable by breaking it into smaller modules [4].

2.2 Bugs in cups with habitrails

As mentioned in the previous section, a key question is whether some network features, such as modularity, affect the stability of networks. Modularity is a feature of networks which describes the clustering of nodes. Networks with high modularity have many connections between nodes in the same module and few connections to nodes in other modules. (See Fig. 2.1.) Early theory predicted that

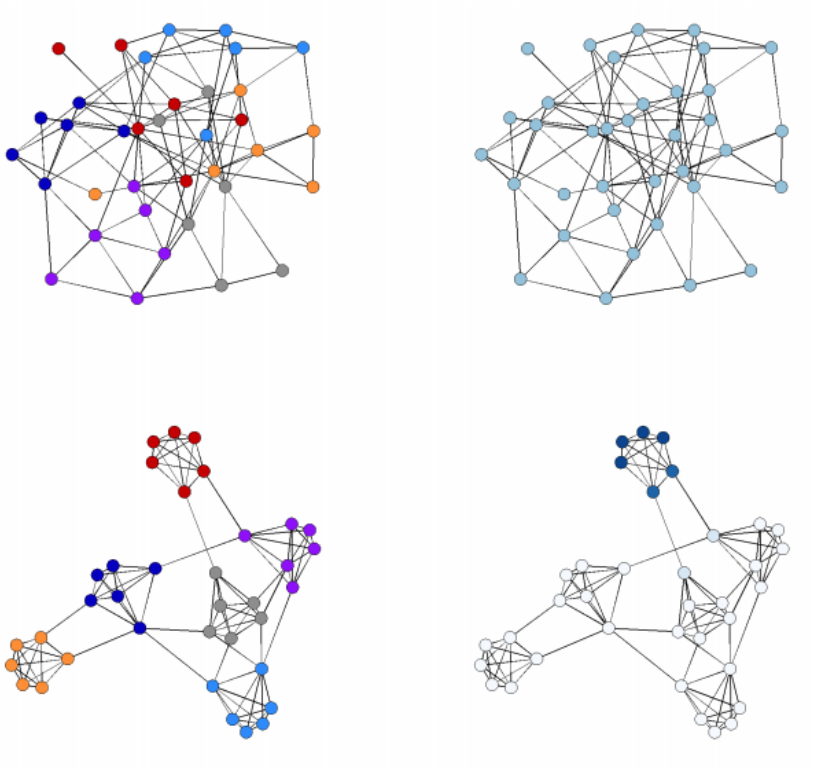

Figure 2.1: Top left: a network with little modularity, with nodes colored. Top right: a network with little modularity, with nodes uncolored. Bottom left: a network with high modularity, with different colors for each module. Bottom right: a network with high modularity, with one module colored.

a modular structure can enhance stability by containing the spread of perturbations. Researchers studying colonies of bats measured the degree of modularity in real networks and used a simple simulation to determine that disease would spread slower in the real-world, modular networks, than in random networks [9].

One of the most relevant papers for this thesis is a recent paper published in *Science*, in which Gilarranz et al. [10] found a correlation between modularity and stability in networks of microarthropods. The "Bugs in Cups" experiment focused on whether modularity can enhance the stability of a network by providing a buffer

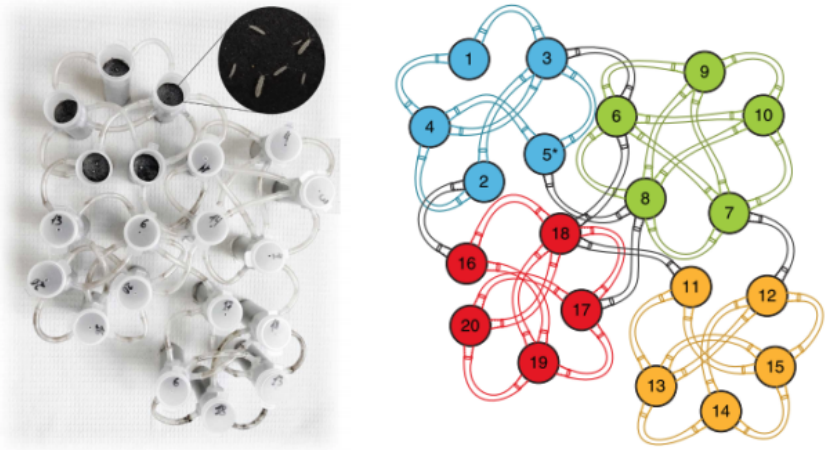

Figure 2.2: Left: vials in the original bugs in cups experiment, with corridors connecting them. Right: a schematic of the vials in the bugs in cups experiment, colored by module.

around a perturbation to isolate damaging effects from the wider network. The experiment tested whether a modular network structure can contain the spread of the impact of a perturbation through time. The experiment employed ten habitat networks, each with large populations of the microarthropod Fulsomia candida, which is a standard arthropod used in ecotoxicology [11]. In the experiment, cups of habitat patches acted as nodes, and movement corridors among the nodes acted as connections to form modules (See Fig. 2.2.). Each node changed population based on the bugs reproducing, dying, and moving to other nodes [12]. Image recognition was used to estimate the dynamics of the changes in population.

After inoculation with a median of 33 bugs in each cup, the local populations grew rapidly until reaching their maximum size [10]. After this growth phase, a perturbation was applied: all bugs were removed from a single node every day for 55 days. The perturbed network was compared with an unperturbed network

(a control). To determine whether the modularity constrains the perturbation, the effects of the perturbation within a module were compared to those in other modules [10]. To measure buffering, the size of the perturbation of each node was calculated. Perturbation size is the number of bugs in the unperturbed network minus the number of bugs in the perturbed network. The buffering ratio is the ratio between perturbation sizes inside and outside the perturbed module [10]. This ratio indicates how many times there are more bugs outside the module versus inside that module. Gilarranz et al. found that the modules confine the spread of the perturbation, which agrees with May's prediction [4] that large systems with high modularities can be more stable.

However, Gilarranz et al. tested only one network structure, and only one node in the network was perturbed. Furthermore, the buffering effect may have been because few bugs were moving between vials in the first place. A more thorough test would be to build an ensemble of networks, with perturbations applied to multiple nodes and varied sharing between nodes, and to vary other parameters as well.

Inspired by this work, we have been studying the effects of perturbations in modular networks in greater detail and with a broader set of analysis tools, including those from nonlinear dynamics.

Chapter 3

Our system and methods

For our work, we are studying networks of interconnected nodes. Our inspiration were several papers on population biology, so we will describe the network and nodes in terms of populations, but because we employ simple models, we expect that much of our work will apply to networks consisting of other types of objects.

3.1 Networks

In this section, I describe how we generate our networks and I provide some description of some network terminology used in this thesis.

3.1.1 Node

A node is an element of the network which can interact with other nodes. In the Gilarranz paper, the nodes were the vials where the bugs lived; another example

might be people in a city. We will use N_n to represent the number of nodes in a network. Just as in the Gilarranz experiment, we have a network of nodes with each node containing a generic "population" which will evolve in a manner described below.

3.1.2 Network structure and connections

Connections

If two nodes are connected, they can exchange population. Two (connected) nodes within the same module form an internal connection, whereas two (connected) nodes from different modules form an external connection.

Degree

A node's degree is the number of connections it has to other nodes in the network. We use k to denote a node's degree of connectivity in the network.

Connection strength

In the networks simulated in this work, if a node is connected to other nodes, it sends a fraction of its population to the connected nodes. The total percentage of population dispersed to other nodes by a single node is the connection strength S. Each node to which it is connected receives S/k percent of the sharing node's population. For all the simulations in this thesis, S is held constant across an

entire network.

May tested connection strength as a parameter and found that increasing S decreased the stability of the network [4].

Geometry

We use the Erdös-Rényi Method, a model to generate a random graph, to create our networks [13]. For each pair of nodes in the network, if the nodes are in the same module, they are connected with probability $Q_{internal}$. If the nodes are in different modules, they are connected with probability $Q_{external}$. The probabilities obey $0 \leq Q_{external} \leq 1$ and $0 \leq Q_{internal} \leq 1$, and in a modular network, $Q_{external} < Q_{internal}$. Once the networks are generated, they are checked to make sure there are no unconnected (or uncoupled) nodes left. Networks with unconnected nodes are discarded. Note that with the Erdös-Rényi method not every node in the network is guaranteed to have the same number of connections.

3.1.3 Modules and modularity

Module

A module is a collection of nodes in a network which are more connected to each other than nodes in other external modules. In the Gilarranz paper, each module contains five cups [10]. In the networks simulated here, the module size is held constant across any given network but may change between trials. We use the

symbol N_m to denote the number of modules in a network.

Modularity

The modularity [14, 15] of the networks is given by the following formula:

$$\mathcal{M} = \sum_{m=1}^{N_m} \left[\frac{l_m}{L} - \left(\frac{d_s}{2L} \right)^2 \right], \tag{3.1}$$

where m runs over each module in the system, l_m is the number of internal connections in each module, L is the total number of connections in the system, and d_s is the sum of the degrees k over nodes in the module. The modularity ranges from -1/2 to 1, with -1/2 representing a network of entirely external connections and 1 representing a network of completely internal connections.

Eq. (3.1) is a standard measure of modularity in networks and some of our results described below reference this measure; however, for convenience, we sometimes use a slightly different measure of modularity — the percentage of connections in the network that are internal:

$$\% \text{ Internal} = \frac{Q_{internal} \left(\frac{N_n}{N_m} - 1 \right)}{Q_{internal} \left(\frac{N_n}{N_m} - 1 \right) + Q_{external} \left(N_n - \frac{N_n}{N_m} \right)}. \tag{3.2}$$

We vary the % Internal from 0.2 to 0.8 in this thesis. A larger value of % Internal usually indicates a more modular network (modularity does not correspond directly to % internal). Fig. 3.1 shows examples of networks with varying degrees

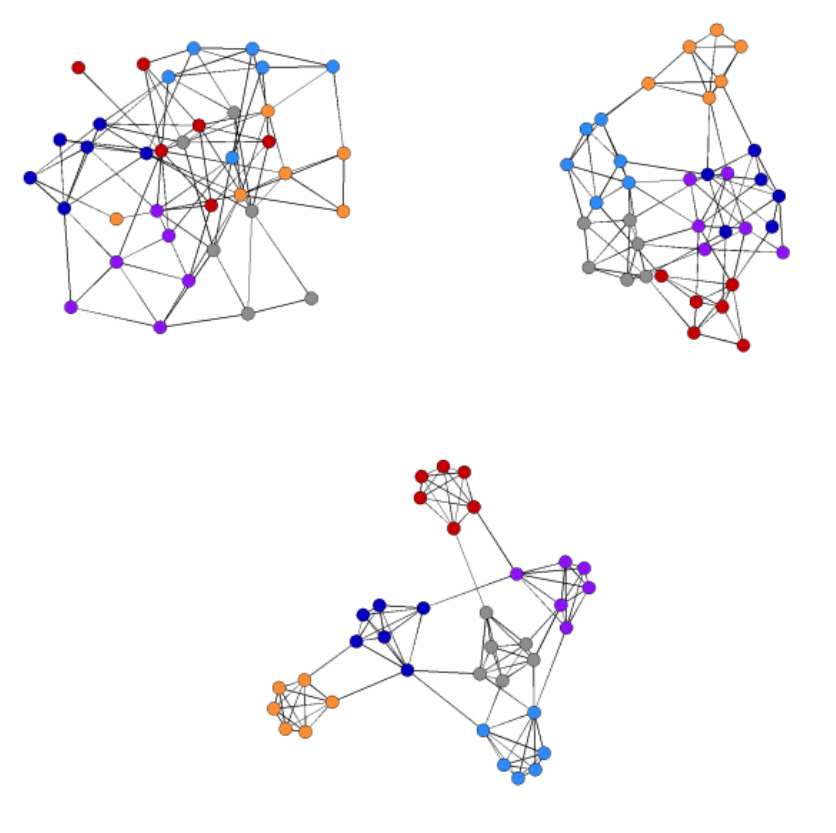

Figure 3.1: Nodes with varying modularity. Top left: a network with little modularity, with nodes colored. Top right: a network with medium modularity, with nodes colored. Bottom: a network with high modularity, with different colors for each module.

of modularity.

3.2 Node population dynamics

Just as in the Gilarranz experiment, we have a network of nodes. (See Fig. 2.1.) The nodes each have a random population between 0 and 1, and the population of each node evolves according to the logistic map:

$$x^{t+1} = f(x^t) = \mu x^t (1 - x^t). \tag{3.3}$$

This is a famous model from population ecology and nonlinear dynamics that is quite simple but exhibits a rich variety of behavior. The equation uses the current population size (x^t) to predict the size (x^{t+1}) after an interval – one year, for example. The parameter μ can be adjusted between 0 and 4. For most values of μ, the asymptotic behavior of the system is either stationary or periodic behavior. Periodic behavior in a discrete dynamical system means the system is in the same state (i.e. x is at the same value) after a set number of iterations.

For example, if we set $\mu = 3.50$, we find period four behavior, and if we set $\mu = 3.52$, we see period eight behavior. For values of $\mu \gtrsim 3.57$, the values bounce around, but x does not return to a previous value. This phenomenon is aperiodic, meaning there is no return to a specified point, and chaotic. An example of this behavior for $\mu = 3.58$ is shown in Fig. 3.2.

Fig. 3.3 shows a section of the bifurcation diagram for the logistic equation. The diagram shows the behavior of the system for various values of the parameter

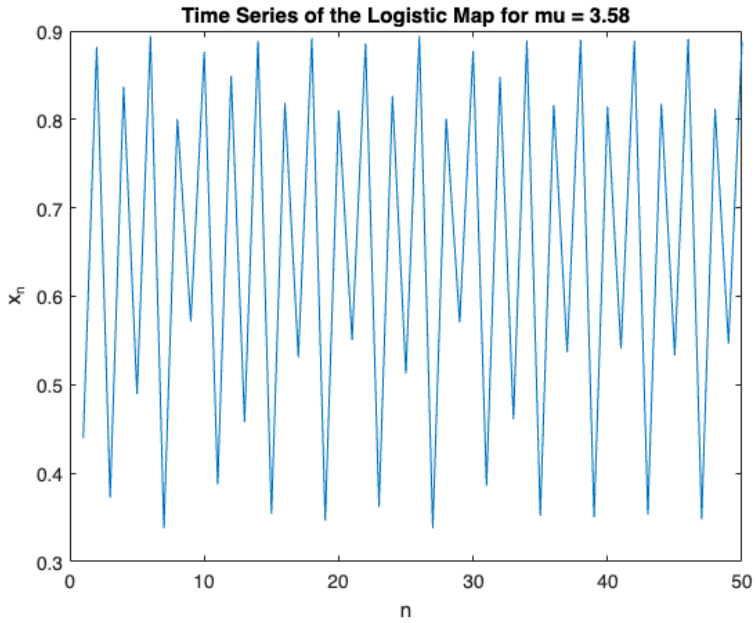

Figure 3.2: Time series of the aperiodic behavior of x_n for $\mu = 3.58$.

μ. For a given μ, the system is evolved from a random value of x^0, and, after a long transient period, all of the subsequent values of x^t are plotted. The figure shows transitions (bifurcations) from fixed point behavior (a point x^* which satisfies $f(x^*) = x^*$) to period two behavior (satisfying $f^2(x^*) = x^*$) to period four behavior (satisfying $f^4(x^*) = x^*$) and so on. After $\mu \gtrsim 3.57$, the behavior is chaotic (except for small windows of periodicity).

Each node in the network is represented by a population (x) between zero and one reflecting a range from zero or a very small population of animals to one or the maximum population of animals in the "node" — that node may be an island, an ant colony, or, in the case of the Gilarranz paper, a cup. Note that in the real world the upper limit on the annual population is not a hard limit, so this is a

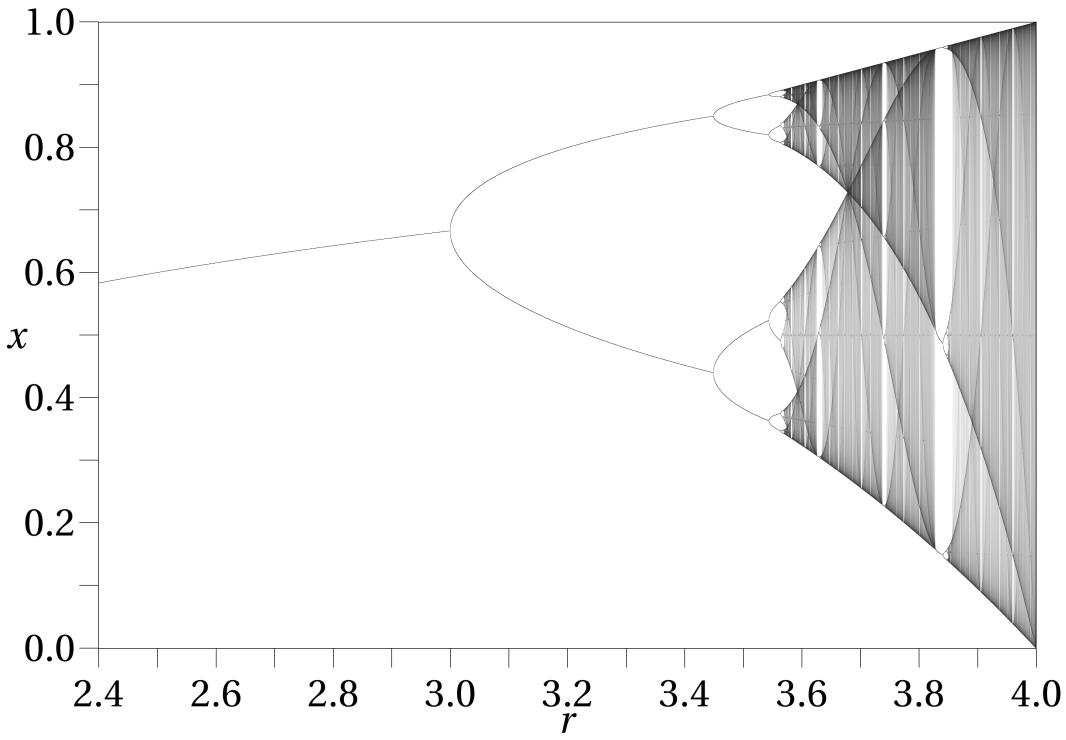

Figure 3.3: Bifurcation diagram for μ vs x. Here μ is denoted r.

simplifying assumption of our model.

The logistic map, Eq. (3.3), is meant to describe the population growth or decrease because of birth and death with the linear term describing reproduction and the nonlinear term describing the suppression of population due to competition for food, etc. This evolution stage does not take into account movement from one node to another, as the inter-node sharing section described below covers this.

3.3 Inter-node sharing

Each node is connected to some of the other nodes and will exchange some of its population with other nodes. This process models the movement of animals or

other examples of population on a node (e.g., sick people, electrical current, or in the Gilarranz example, *Folsomia*) from one node to a connected node. Each node sends a percentage S of its population to nodes connected to it. Thus each of the k nodes to which it is connected receives the same population. For each node i, the connected nodes are indexed as $j = 1, 2, ..., k_i$, and the new value of the population at node i at iteration $t + 1$ is determined by:

$$x_i^{t+1} = (1 - S)f(x_i^t) + \sum_{j=1}^{k_i} \frac{S}{k_i} f(x_j^t), \tag{3.4}$$

where $f(x)$ is the logistic map, Eq. (3.3), and where the first term represents sharing and the second receiving. In this thesis we vary S from 0.01 to 1 by increments of 0.01.

The node sharing interaction does not preserve the total population of the network, however. A node with comparatively few connections will give away more population to a node with many connections than the second node receives, and a node with many connections gives away less population than a node with relatively few connections receives. Since the number of connections varies in the Erdös-Rényi method, total population is not conserved. However, the advantage of this population sharing method is that it keeps the population of each node between 0 and 1, a necessary condition for the logistic equation to produce positive numbers.

3.4 Nonlinear dynamical analysis

Now that we have our system and its evolution, we can introduce the measures used to analyze stability and dynamics, which come from the science of nonlinear dynamics and chaos. The buffering effect studied by the Gilarranz group in their experiments relies on repeated perturbations of a single node; however, there are many ways to perturb a system, and not all ways will lead to the same behavior. For more broadly applicable results, in this work we use a tool set that can handle a wider range of perturbations. This tool set exists in nonlinear dynamics and chaos theory. Lyapunov vectors, Lyapunov exponents, Lyapunov dimensions, and vector participation ratios are measures that are commonly used to characterize stability and instability in dynamical systems [16–25].

3.4.1 Lyapunov vectors and exponents

A Lyapunov vector represents a way in which a small (actually, infinitesimal) perturbation can be applied to the network. For example, the entire perturbation can be applied to a single node, as in the Gilarranz experiment. The vector for this perturbation would be $(0, 0, 0, 1, 0, \ldots, 0)$, where the non-zero component represents the perturbed node. The other extreme is the perturbation being applied evenly across the entire network, with each node gaining or losing the same amount of population. The vector for this perturbation would be $C \cdot (1, 1, 1, 1, 1, \ldots, 1)$, where C is a normalization factor. Each vector has N_n components where each

component represents one node in the network. Together, all the vectors form an orthonormal basis, so any perturbation can be written as a linear combination of the N_n Lyapunov vectors.

We rank the Lyapunov vectors according to how quickly a perturbation with the given distribution would grow in magnitude. The first vector describes the perturbation with the fastest growth rate over long times. Because the vectors form a basis, all other vectors must be orthogonal to the first. The second vector describes the fastest growing perturbation possible that does not contain any projection of the first vector and so forth.

The average growth rate of each Lyapunov vector is measured by the Lyapunov exponent [26]. The magnitude of each Lyapunov vector $\mathbf{v}$ grows on average as:

$$||v(t)|| = ||v(0)||e^{\lambda t}, \tag{3.5}$$

where λ is that vector's Lyapunov exponent, and t is the number of iterations. The first vector, as the fastest growing mode, has the largest exponent, the second vector has the second largest exponent, and so forth. The exponents describe whether the network behaves chaotically. If the first Lyapunov exponent is negative, any possible perturbation to the network will disappear over time, and the network eventually settles to a periodic or to a steady state. If the first exponent is positive, then even very small perturbations will grow, and the network will behave aperiodically.

To calculate the Lyapunov vectors and exponents numerically, we do not actually directly simulate a perturbed system and compare it to an unperturbed system. If we did that, we would be applying finite perturbations instead of infinitesimal perturbations, and the two systems could quickly become uncorrelated; at that point, we would not be measuring properties of the underlying, unperturbed system. Instead, we study the tangent space of the system by determining the dynamical equations governing the evolution of the perturbations themselves [27].

Since our nodes are connected in a linear fashion using Eq. (3.4), we can calculate the growth of perturbations on each node using the logistic equation, Eq. (3.3), and then couple the nodal perturbations together using an equation similar to Eq. (3.4). In particular, for an infinitesimal perturbation δx_i to population x_i on node i, the perturbed population will evolve according to Eq. (3.3) as:

$$\begin{aligned} f(x_i + \delta x_i) &= \mu\,(x_i + \delta x_i)(1 - (x_i + \delta x_i)) \\ &= \mu\,(x_i - x_i^2 - x_i\delta x_i + \delta x_i - x_i\delta x_i - \delta x_i^2) \\ &= \mu\,(1 - x_i) + \mu\,\delta x_i(1 - 2x_i - \delta x_i) \\ &= f(x_i) + \mu\,\delta x_i(1 - 2x_i - \delta x_i), \end{aligned}$$

so, keeping only terms to linear order in δx_i since the perturbation is infinitesimal,

$$f(x_i + \delta x_i) - f(x_i) \approx \mu\,\delta x_i(1 - 2x_i) \equiv g(x_i, \delta x_i). \tag{3.6}$$

This equation directly describes the evolution of an infinitesimal difference between a perturbed population and an unperturbed population on an unconnected node.

Now, we need to couple the perturbations from the various nodes together using their connections and the connection strength S (similar to Eq. (3.4)) to get the final evolution equations for the Lyapunov vectors:

$$\delta x_i^{t+1} = (1 - S)g(x_i^t, \delta x_i^t) + \sum_{j=1}^{k_i} \frac{S}{k_i} g(x_j^t, \delta x_j^t). \tag{3.7}$$

Our networks are described by N_n Lyapunov vectors each evolving according to Eq. (3.7). Because the first Lyapunov vector describes the evolution of the fastest growing perturbation, we can actually start with almost any perturbation and it will quickly align itself with the true first Lyapunov vector. Unfortunately, because of numerical noise, that also means that all N_n of our Lyapunov vectors will tend to align with each other over time instead of remaining orthogonal, unless we intervene. We keep the vectors orthogonal by using a modified Gram-Schmidt orthogonalization procedure. In the Gram-Schmidt procedure, orthogonalized vectors are calculated as:

$$\vec{u}_{ortho} = \vec{u} - \sum_j \left(\frac{\vec{u} \cdot \vec{v_j}}{\vec{u} \cdot \vec{u}} \right) \vec{v_j}, \tag{3.8}$$

where $\vec{v_j}$ are the vectors with smaller exponents. However, we use the modified Gram-Schmidt process, in which the order of subtraction is reversed: after each vector is calculated, its projection onto less optimal (lower exponent) vectors is

subtracted from those vectors. The Gram-Schmidt and modified Gram-Schmidt processes are theoretically equivalent, but the modified process is more numerically stable than the traditional process.

The finite-time Lyapunov exponents are calculated at each time step as:

$$\lambda^{(1)} = \ln \frac{||u^{t+1}||}{||u^t||} \tag{3.9}$$

for each Lyapunov vector u. The (infinite-time) Lyapunov exponent is just the average of the finite-time exponents over long times [27]. A positive Lyapunov exponent means on average the perturbation grew, and this is the hallmark of an unstable (or chaotic) network. A negative Lyapunov exponent means on average the perturbation shrank. If all of the Lyapunov exponents are negative then the network is stable. To give an idea of scale, the average Lyapunov exponent for a slightly chaotic μ value of 3.58 is roughly 0.06, meaning it would take about $1/0.06 \approx 17$ iterations for a perturbation to grow by an order of magnitude.

3.4.2 Inverse participation ratio

The node inverse participation ratio for a normalized Lyapunov vector $(x_1, x_2, x_3, ..., x_{N_n})$ is calculated as according to the following equation:

$$PR_n = \left(\sum_{i=1}^{N_n} (x_i)^4 \right)^{-1}.$$

This number characterizes the number of nodes participating strongly in the Lyapunov vector. We will illustrate the properties of participation ratios with a few examples. If a vector is concentrated completely in a single node, $\hat{v} = (1, 0, 0, 0, ...)$, then the participation ratio will be one:

$$PR_n = (1 + 0 + 0 + ...)^{-1} = 1.$$

If the vector is evenly distributed among two nodes, $\hat{v} = (\sqrt{\frac{1}{2}}, \sqrt{\frac{1}{2}}, 0, 0, ...)$, then

$$PR_n = (0.25 + 0.25 + 0 + 0 + ...)^{-1} = 2.$$

If the vector is evenly distributed among all N_n nodes, $\hat{v} = (\sqrt{\frac{1}{N_n}}, \sqrt{\frac{1}{N_n}}, \sqrt{\frac{1}{N_n}}, \sqrt{\frac{1}{N_n}}, ..., \sqrt{\frac{1}{N_n}})$, then

$$PR_n = (N_n \cdot \frac{1}{N_n^2})^{-1} = N_n.$$

3.4.3 Modified inverse participation ratio

The inverse participation ratio described above characterizes the spread of the Lyapunov vector at a moment in time, but Lyapunov vectors evolve over time, and at a given time a perturbation might be more localized on one node and at another time the perturbation might be more localized on another node. If we are interested in how many nodes are affected by a perturbation over a longer period of time, then we can calculate a modified inverse participation ratio. To do this,

we average the magnitudes of the nodal contributions to the Lyapunov vector over long times (typically 50,000 iterations) and then calculate the inverse participation ratio of this average Lyapunov vector. The modified participation ratios tell us how well spread the perturbation is over the whole network in a long period of time.

3.4.4 Modular inverse participation ratio

To characterize how well-localized the Lyapunov vector is to various modules, we calculate a quantity we call the modular inverse participation ratio. This measure is calculated in a similar manner to the nodal inverse participation ratio:

$$PR_m = \left(\sum_{j=1}^{N_m} \left[\sum_i x_i^2 \right]^2 \right)^{-1},$$

where j iterates over the modules in each network and i iterates over the nodes in each module. This quantity characterizes over how many modules the Lyapunov vector is spread.

3.4.5 Percent of contribution in largest module

The percent of the contribution in the largest module is a measure of how contained the system is by its modularity. It is meant to test the claim that modularity can add stability to a network by localizing perturbations. Higher percent of contribution in largest module means the network's perturbation modes are constrained

to one module and don't spread much to nodes in other modules. It is calculated as the largest sum of node Lyapunov contributions among all modules.

3.4.6 Percent of networks with positive exponents

We typically perform calculations on an ensemble of 100 networks, each with the same parameters but generated using a different random seed and thus with different connection geometries. Because of the differences in connections, the dynamics on the networks can differ. We calculate the percent of networks with positive exponents in order to see whether networks behaving stably on average are in fact sometimes unstable and are being skewed by negative results. To compute the percent of networks with positive exponents, we simply add the number of networks which have positive exponents and divide by 100 networks.

3.5 Variance

The variance among the ensemble of 100 networks is shown in the results after every graph. High variance is a marker of a phase change in statistical physics. Similarly, in our system higher variance seems to indicate that a change is about to occur, usually a change in the measure's values as a result of an increase in the connection strength S.

The error bars are a form of standard deviation, or $\frac{\Sigma(\sigma-\bar{\sigma})^2}{\sqrt{N}}$ where σ is the particular quantity we measure (such as participation ratio or first Lyapunov ex-

ponent) and N is the number of networks, and where the sum is averaged over all the networks. The size of the error bars provide a measure of how similar the networks are given that they have the same modularity within 0.01 (the modularity is unitless).

3.6 Computational parameters

Besides the structural parameters used to construct the networks (% Internal or modularity, number of nodes, number of modules), the parameter that characterizes the interactions between nodes (connection strength S), and the logistic map parameter μ, the only other parameters are the transient length, the collection period, and the ensemble size.

As mentioned above, we typically use an ensemble of 100 networks all generated with the same structural parameters.

For each simulation of a network, the initial population values on the nodes are assigned at random between one and zero. We also assign random values to the Lyapunov vector components. We then evolve the system through a transient period of 50,000 iterations to allow the system to reach a statistically stationary state and to allow the Lyapunov vectors to align with their asymptotic directions. After the transient period, we then collect data for 50,000 iterations to perform averaging. Sample ensembles with runs of 10 times as many iterations were used to ensure that the transient duration was long enough and that measured values

converged.

Chapter 4

Results

We note first that the phenomena shown on the figures below are still to a large extent unexplained; thus, in this results section I devote most of my writing to describing our research and our current understanding of chaotic-node networks and their behavior as we vary modularity, degree of connectivity, and size of the network. Our networks each have chaotic growth (or decay) of their node populations, and in most figures connection strength S (how much population the nodes share with each other) is varied on the x axis. We also vary the modularity of the system in most figures in order to compare networks which are highly connected in groups, to those which have the same number of connections but more random distribution of those connections throughout the network.

4.1 Lyapunov Exponents

Lyapunov exponents are a measure of how stable or unstable a system is. Positive exponents indicate instability, with larger exponents indicating greater sensitivity to perturbations, whereas negative exponents indicate stability, with smaller exponents indicating that perturbations die out more quickly.

In Fig. 4.1, we show the first Lyapunov exponent λ_1 as a function of connection strength S for a variety of modularities for $\mu = 3.58$. For small to moderate values of the modularity ($\mathcal{M} \lesssim 0.5$), the results broadly support May's claim [4] that higher modularity leads to more stability since the exponents are lower as modularity is increased. For larger values of the modularity, the situation is more complicated, and the increased modularity can actually lead to greater instability in networks.

We note that these data are collected using a value of $\mu = 3.58$ in Eq. (3.3), which is past the point in the bifurcation diagram where the system has infinite period doubling and so individual unconnected nodes would display chaos. In particular, if each node was not connected to any other nodes, we would expect that the nodes would be characterized by a Lyapunov exponent of ~ 0.105. Indeed, with small connection strength we see that the Lyapunov exponent is very close to 0.105, which we expect because there is not much population sharing from node to node (i.e. there is not much deviation from the original behavior of the logistic map).

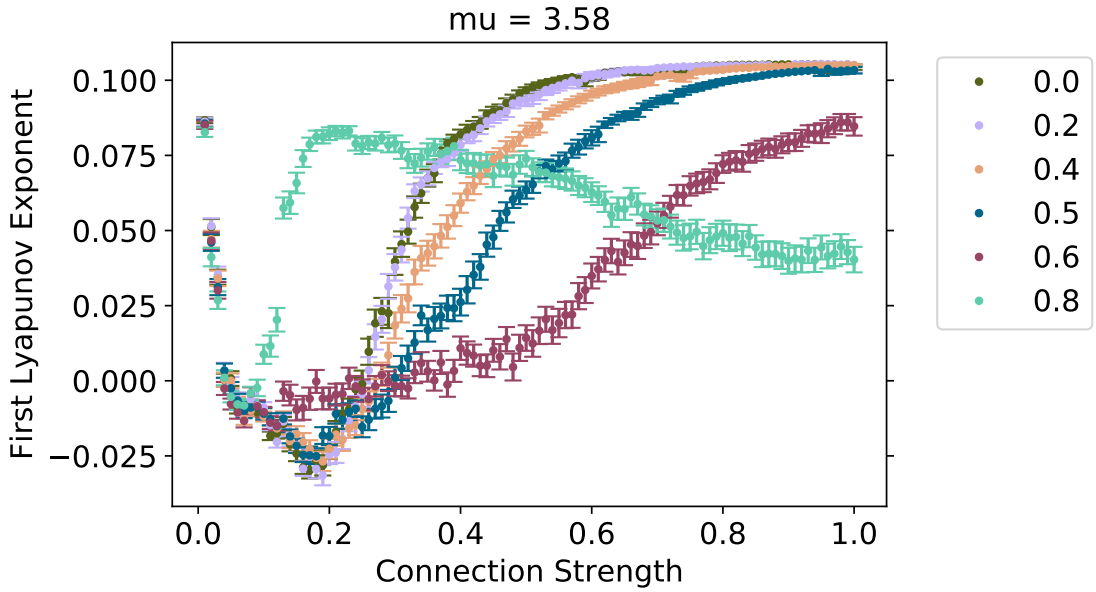

Figure 4.1: First Lyapunov Exponents. The 0.8 modularity ensemble are the most modular systems, whereas the 0.0 modularity ensemble are the least modular ones. The networks in each ensemble have 8 modules ($M = 8$), 8 nodes per module ($N = 8$), an average of 4 connections per node ($k = 4$), and $\mu = 3.58$

When there is just a bit more sharing ($0.05 \lesssim S \lesssim 0.25$), however, the system surprisingly stabilizes, at least for $\mathcal{M} \lesssim 0.6$. This is intriguing since the underlying dynamics on each node is chaotic. It appears as though the intermediate connection strength somehow stabilizes networks whereas larger connection strengths make the system more chaotic. To explain the decrease in λ_1 and the stability in the initial connection strength values, we look to Eq. (3.4):

$$x_i^{t+1} = (1 - S)f(x_i^t) + \sum_{j=1}^{k_i} \frac{S}{k_i} f(x_j^t),$$

where $f(x)$ is the logistic map, Eq. (3.3), and where the first term represents sharing and the second receiving. An increase in the connection strength effectively

lowers the μ factor in the front. The right hand term represents an average, so any chaotic behavior for individual nodes decreases (because we average over all connected nodes). This means instead of restoring the μ factor to its original value, the second term makes the μ value we observe slightly less. As we increase S, then, we decrease $\mu_{effective}$. In Fig. 4.1, we observe behavior consistent with a new effective μ :

$$(1 - S)\mu < \mu_{effective} < \mu \tag{4.1}$$

Looking at the bifurcation diagram (Fig. 4.2), we see that the chaos becomes less when we decrease μ (there denoted r), and then enters into periodic behavior for $\mu \lesssim 3.57$. We can observe similar behavior for a single node's population in one network; in Fig. 4.2 on the right, notice the chaotic behavior (indicated by a continuum of values the equation takes on) for low connection strengths ($S \lesssim 0.02$) and the periodic behavior for $S \gtrsim 0.03$, which eventually turns into period-4 behavior and then period-2 behavior. This period-halving compares to the graph on the left of Fig. 4.2, where for $\mu = 3.58$ we observe chaos, for $\mu = 3.55$ there is period-8 behavior, for $\mu = 3.45$ there is period-4 behavior, and for $\mu \gtrsim 3$ there is period-2 behavior. For $S \gtrsim 0.2$, the node populations plotted on the right of Fig. 4.2 revert to higher period behavior and eventually go back to chaos as S increases. For $S > 0.2$, the nodes share much more, meaning they are no longer independent. This is why the period starts doubling and why chaos happens for

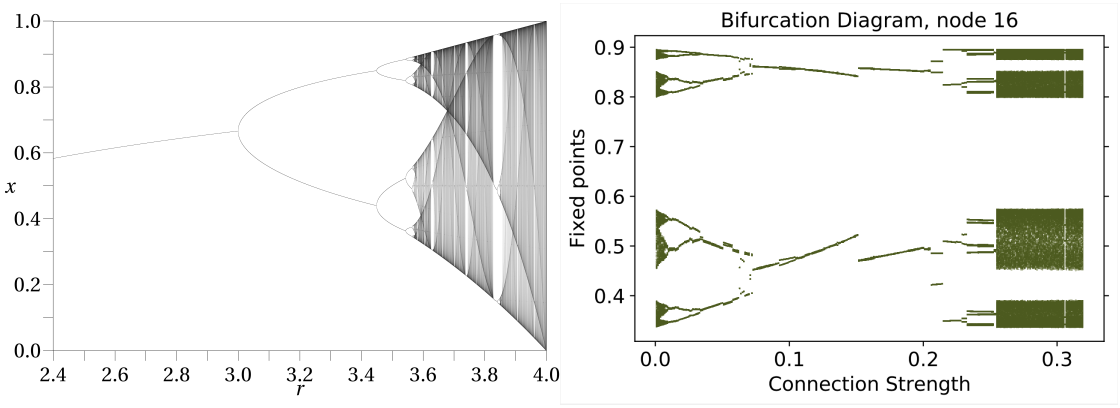

Figure 4.2: Bifurcation Diagrams. Left: Bifurcation diagram for μ vs x, where μ is denoted r. Right: Bifurcation diagram for one node's population in a single network. The network has $\mu = 3.58$ (and modularity 0.4), but as connection strength is increased, it is as if μ decreases to

larger connection strength values. In conclusion, when we observe stable behavior for an unstable parameter ($\mu = 3.58$), this comes from node sharing which changes the effective value of μ.

We have also tested a higher value of μ to see if a similar phenomenon occurs. In particular, we tested $\mu = 3.84$, a value which gives period-6 behavior in the logistic map. We expect that a small amount of sharing will create a smaller $\mu_{effective}$, pushing the system into the chaotic region of the bifurcation diagram. Observe in Fig. 4.3 the positive Lyapunov exponents, which indicate (in agreement with our theory) that the system has shifted from period-6 to chaotic behavior. Moreover, as the connection strength is increased, the system becomes less chaotic, which aligns with a leftward shift in the bifurcation diagram from 3.84 (as μ gets lower from 3.828, the chaos in the logistic map's populations decreases). One may wonder why there is no shift from stable behavior to chaotic behavior (i.e. why

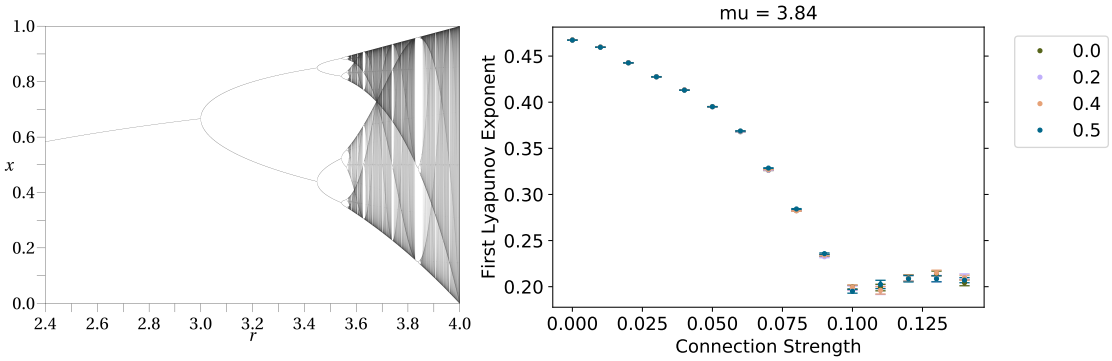

Figure 4.3: Left: Bifurcation diagram for μ vs x, where μ is denoted r. Right: First Lyapunov Exponent vs. Connection Strength for $\mu = 3.84$. Similarly to in the $\mu = 3.58$ case, we see a $\mu_{effective}$ less than the inputted μ and a decrease in $\mu_{effective}$ as S increases.

there are no negative Lyapunov exponents for very low connection strength). This is because a very small amount of sharing leads to chaotic behavior. Indeed, the values shifted from being stable to being chaotic at an S value of around S=0.005. So in this case, we start with stable dynamics, but after a very small amount of sharing, the system becomes chaotic.

Synchronized Chaos

The cases we have just discussed are for low sharing. With more sharing, the system behaves like we might expect – it becomes unstable. Eventually, the system develops global behavior with the network returning to the original value of the Lyapunov exponent. Based on visualizations of the dynamics of individual networks, the system has synchronized such that the entire network behaves as one node. We note that this behavior is different from the very low connection strength behavior even though the values of λ_1 are similar — in networks with very low

sharing, each node is virtually independent.

In the high sharing region of Fig. 4.1, all the nodes have the same value, and the system behaves like a single (albeit chaotic) node. We can prove that if one node diverges a small amount from the other nodes' values, the node will converge back to the other nodes' value. Here is the analytic approach we use:

A synchronized chaotic state is stable to independent single-node perturbations if a perturbation to one node shrinks. We can add a small perturbation term δ_{x_i} to Eq (3.4) in the following manner:

$$f(x_i + \delta_{x_i}) = (1 - S)\mu(x_i + \delta_{x_i})(1 - x_i - \delta_{x_i}) + S\mu x_i(1 - x_i)$$

Where the other nodes are synchronized, meaning the second term in Eq (3.4) adds to $S\mu x_i(1 - x_i)$.

This simplifies to

$$f(x_i+\delta_{x_i}) = (1-S)\mu(x_i)(1-x_i)+(1-S)\mu x_i(-\delta_{x_i})+(1-S)\mu\delta_{x_i}(1-x_i)+S\mu x_i(1-x_i)+\text{terms in } \delta_{x_i}^2$$

$$f(x_i + \delta_{x_i}) \approx f(x_i) + (1 - S)\mu(\delta_{x_i})(1 - 2x_i)$$

So this single-node perturbation will shrink if

$$(1 - S)\mu|1 - 2x_i| < 1.$$

For $\mu = 3.58, 0.3 \lesssim x_i \lesssim 0.9$, so $\max|1 - 2x_i| \approx 0.8$

So the perturbation will shrink for $S = 1 - \frac{1}{\mu|1-2x_i|} \approx 0.65$

Modularity of 0.8

Another interesting aspect of Fig. 4.1 is that for the modularity of 0.8, there is a maximum value of λ_1 at a connection strength of $S = 0.20$. This indicates that the system is behaving most chaotically when it is in an intermediate value of S, quite different from the behavior at lower modularities. This observation contradicts our intuition in several ways: firstly, the Lyapunov exponent of a modular network seems like it should be less than that of a non-modular network (as May [4] predicted), but between $0.05 \lesssim S \lesssim 0.75$, the λ_1 values for $\mathcal{M} = 0.8$ are higher than those for at least some smaller modularities. Secondly, May [4] predicted that stability should decrease with larger connection strength S; however, for $\mathcal{M} = 0.8$, λ_1 is decreasing with increasing S, indicating that the networks are becoming less unstable.

Further Analysis of Lyapunov Exponents

An interesting observation of the Lyapunov exponents is that the various modularities appear to cluster into three qualitatively-similar behavior types. We checked 18 different modularities and they all aligned with each other in one of three ways (see Fig. 4.1): modularities below 0.4 have very little difference from each other; they exhibit stable first Lyapunov exponents for $0.05 \lesssim S \lesssim 0.25$ with λ_1 rising

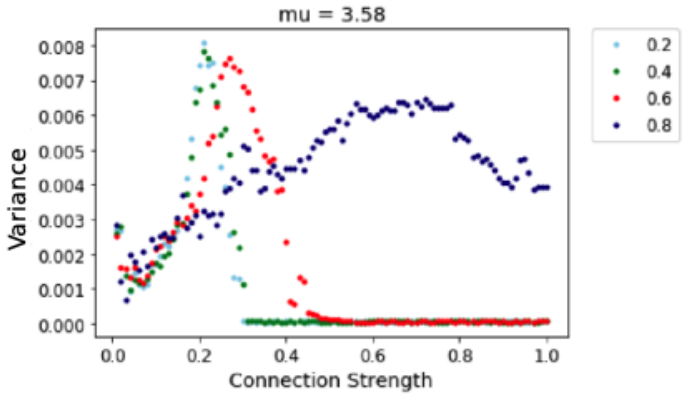

Figure 4.4: Variance of measurements of λ_1. Legend: Percent Internal runs from 0.2 to 0.8.

quickly toward its maximum value after that. This indicates that the modularity below 0.4 has little effect for average connectivity (k) of 4. However, looking at the differences between the modularity of 0.4 and the modularity of 0.6, we see that instead of a dip and a dramatic rise, λ_1 for $\mathcal{M} = 0.6$ has a broad plateau of marginal stability ($\lambda \approx 0$) for $0.05 \lesssim S \lesssim 0.6$. This is true for all modularities we tested between 0.5 and 0.65. For modularities higher than 0.8, we see the modularity graphs all have the same behavior: a dip around $S = 0.1$ followed by a steep incline around $S = 0.2$ where λ_1 reaches its maximum, and a steady linear decline for higher connection strength values. Three behaviors are apparent for varying modularity: a dip and then steep rise to the maximum possible value, a broad plateau of marginal stability, and a maximum before decreasing.

We note that the error bars in Fig. 4.1 are larger in the transitional region from $S \approx 0.2$ to $S \approx 0.4$. To make this more apparent, in Fig. 4.4, we've plotted the variance in the measurements of λ_1 for the 100 networks in our ensemble. The

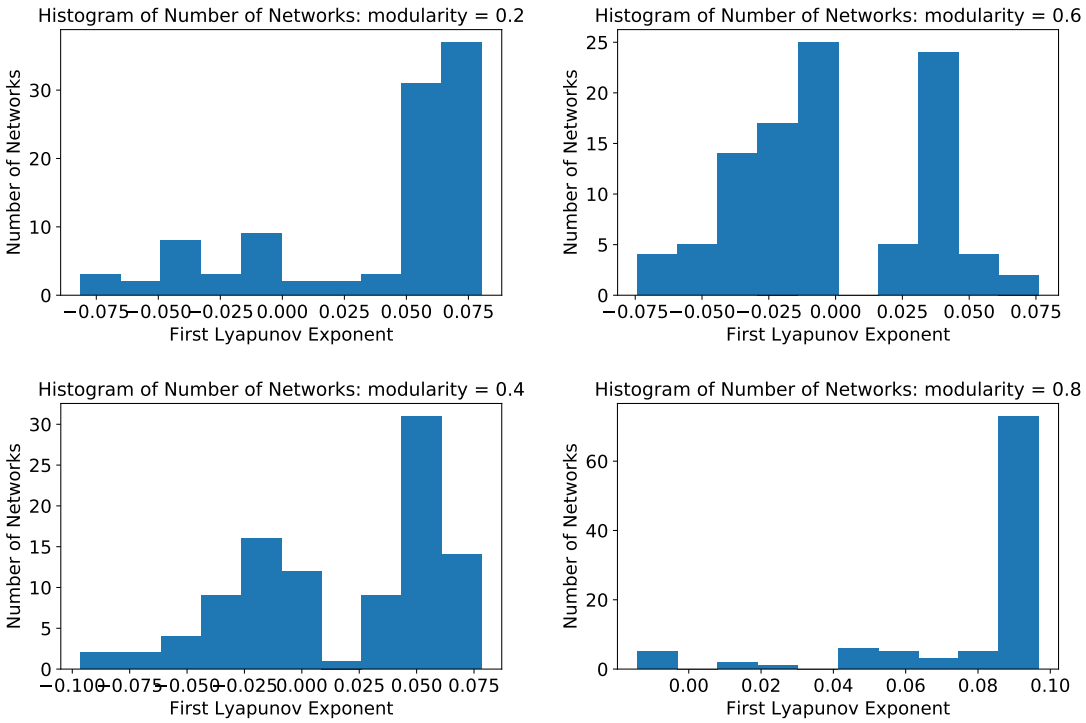

Figure 4.5: Histograms of first Lyapunov exponents for varying modularities and connection strength ($S = 30$) in the early transition region. Degree of connectivity is varied, and the other parameters are kept at the defaults ($k = 4, M = 8, N = 8$.)

larger variance, a factor of 8 times larger than the variances at very-low S, indicates that our networks behave in a wide variety of ways for the same parameters. We note that an increase in variance is often indicative of a transition in statistical mechanics, here possibly indicating a transition between local and global behavior.

To explore what is happening in the transitional region, we plotted histograms of λ_1 for the ensemble of networks for a connection strength of $S = 0.30$. These are shown in Fig. 4.5. We see that the distributions, especially for $\mathcal{M} = 0.4$ and $\mathcal{M} = 0.6$, are bimodal, likely indicating two distinct behaviors within the ensemble: some networks are stable with $\lambda_1 \approx -0.025$ and other networks are unstable with

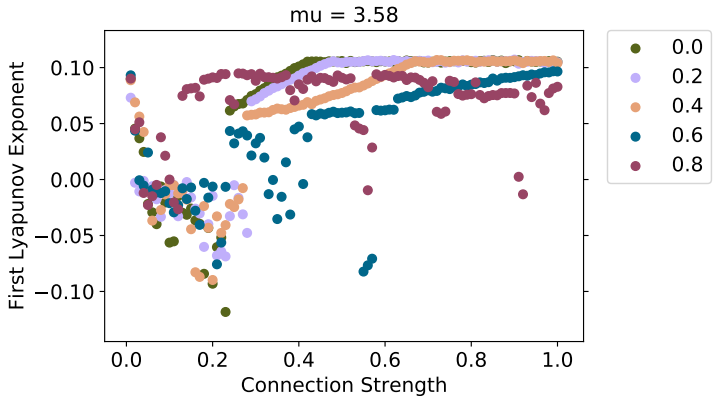

Figure 4.6: Top Left: exponents for $k = 4, M = 8, N = 8$. Legend: modularity runs from 0.0 to 0.8.

$\lambda \approx 0.05$.

This bimodal behavior in Fig. 4.5 suggests that individual networks might make a discontinuous transition between stable behavior and unstable behavior. We have plotted λ_1 vs. S for many individual networks, and an example of this is shown in Fig. 4.6. We see that for $\mathcal{M} <= 0.4$ and, possibly $\mathcal{M} = 0.8$, there is a distinct jump in exponent at a specific value of S, indicating a discontinuous change in dynamics, rather than a smooth transition.

For different networks, we have noted that the transition points in S vary, even for the same modularity. This is not unexpected since each network has a unique geometry. We believe these varying transition points lead to the smooth rise in λ_1 vs. S in Fig. 4.1, obscuring the underlying discontinuities in the dynamics.

4.2 Inverse Participation Ratios

As discussed above, the first Lyapunov vector describes the perturbation that would grow the fastest over long times. This is the perturbation to which the system is most susceptible. An inverse participation ratio of X means the perturbation mode is centered on X nodes. (For convenience, I will often drop the "inverse" in the discussion below.) We see from Fig. 4.7 (top left) that with very low connection strength S (with S running from 0.01 (1% sharing) to 1.00 (100% sharing)), only one node experiences the perturbation. However, with very high connection strength ($S > 0.75$), many more nodes participate in the perturbation, meaning the participation ratio is much higher. In particular, for a modularity of 0, 0.2, or 0.4, by the high S values, all or nearly all nodes are participating in the largest perturbation — the system is susceptible to a global instability.

In Fig.4.7 (top left), we show the inverse participation ratio as a function of S for modularities ranging from $\mathcal{M} = 0.0$ to $\mathcal{M} = 0.8$ and $\mu = 3.58$. For $\mathcal{M} \lesssim 0.6$, there is a fairly dramatic transition between small participation ratios and large ones over a small range of S values. Similar behavior can be seen in Fig. 4.7(bottom left) for the modular inverse participation ratios.

Because we thought this transition might only look continuous on average but truly be discontinuous for individual networks in our ensemble, we wanted to see what happens in the transition region, $0.25 < S < 0.75$, where on average the participation ratio is neither 1 nor 64 (the number of nodes in the system), but

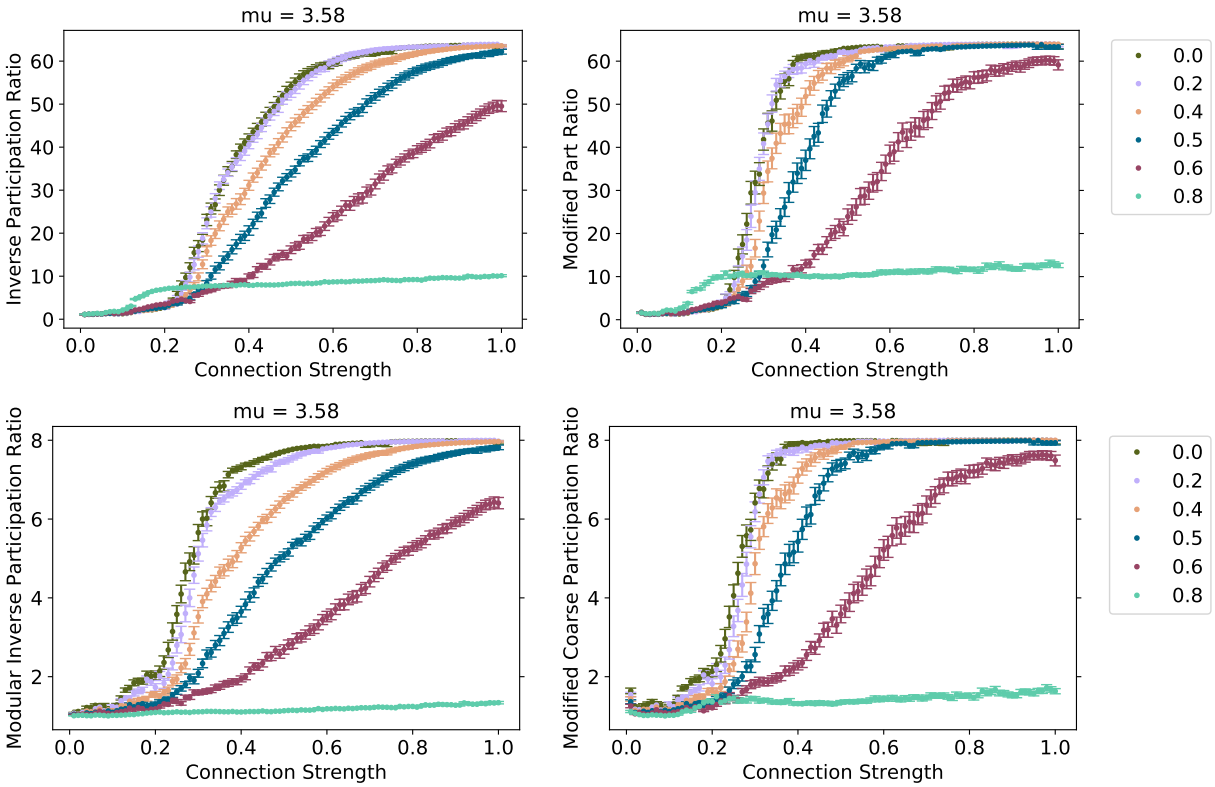

Figure 4.7: Top Left: inverse participation ratios averaged over each ensemble of networks. Bottom Left: modular inverse participation ratios. Top Right and Bottom Right: the modified counterparts of the inverse participation and the modular (coarse) inverse participation ratios, respectively. The legend shows the modularity of the systems (each network in the ensemble has a modularity within 0.01 of the number shown). The 0.8 modularity ensemble are the most modular systems, whereas the 0.0 modularity ensemble are the least modular ones. The networks in each ensemble have 8 modules ($M = 8$), 8 nodes per module ($N = 8$), an average of 4 connections per node ($k = 4$), and $\mu = 3.58$.

in-between 1 and 64. Was there a smooth transition between the localized perturbation and the global perturbation, wherein several but not all nodes were participating, or was there a sharp transition when all the nodes in the system suddenly started participating in the Lyapunov vector? In Fig. 4.8(top left), we show a histogram of the inverse participation ratios for the 100 different networks in our ensemble, each for modularity $\mathcal{M} = 0.2$ and for $S = 0.30$. We see that the histograms of individual networks are bimodal. There are two behaviors where the networks tend to align: one behavior is global and the other is local. There are few networks in the in-between region for a modularity below 0.4; for a modularity of 0.2, 80% of the networks are either below 2 or greater than 25. Similarly, for a modularity of 0.4, 71% of the networks are either below 2 or greater than 20. This bimodal behavior again suggests that networks are discontinuously transitioning from low to high participation ratios at a certain connection strength which differs for each network.

This interpretation that individual networks undergo a fairly rapid transition from localized to global instability is supported by Fig. 4.9(top left), which shows an example of the inverse participation ratio as a function of S for a single network. For small values of $\mathcal{M}$, we see a rapid transition from a localized mode to a global mode.

We also computed a modified participation ratio (described above in Sect. 3.4.3) to monitor the spread of perturbations over time rather than simply looking at the

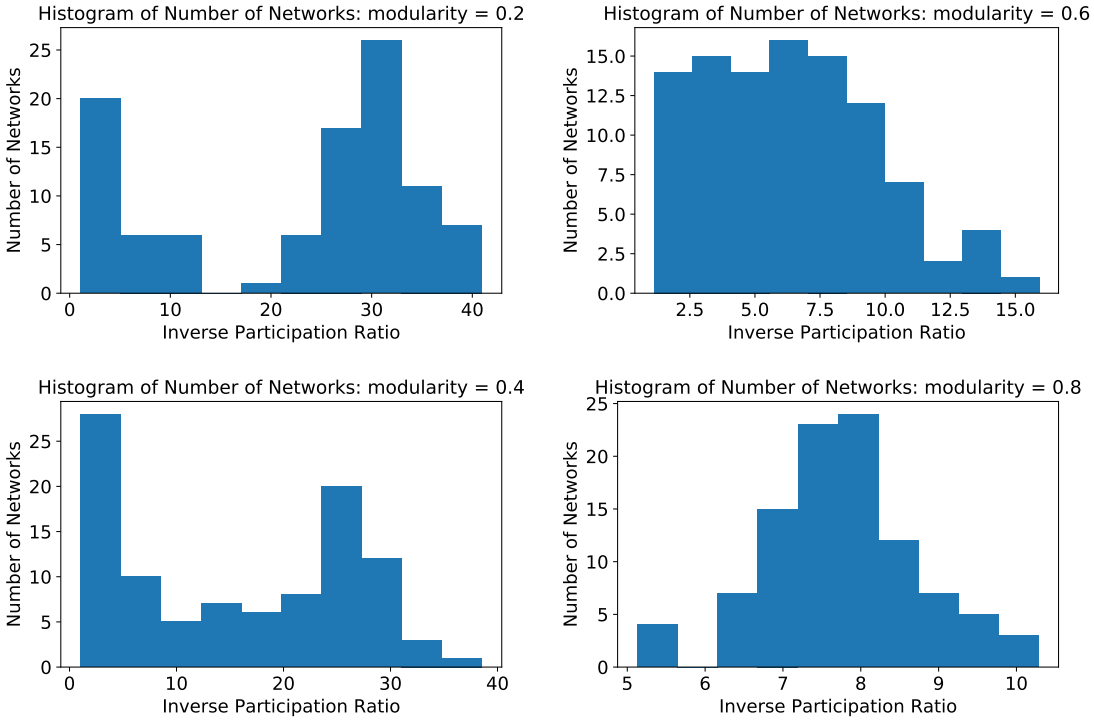

Figure 4.8: Histograms of inverse participation ratio for varying modularities and connection strength ($S = 0.30$) in the early transition region. Modularity is varied, and the other parameters are kept at the defaults ($k = 4, M = 8, N = 8$).

average extent of the Lyapunov vector at each time step. If we have a perturbation that is constrained to, say, 8 nodes at one time, it may be the case that the perturbation will be localized on another 8 nodes at another time. Thus, the inverse participation ratio will be 8 for each and the average will be 8. However, by averaging the vectors after all the time steps and then computing an inverse participation ratio on that average vector, we would find a larger value (16, if the perturbation spends equal time on the two groups of 8 nodes in the example). We have observed two scenarios for perturbations: one in which the perturbation remains roughly centered on one set of nodes the entire time, and the other in which the perturbation moves around over time "leaking" from one group of nodes to another. Most importantly, our modified participation ratio can detect when perturbations spread globally even when only a smaller number of nodes are involved at any given moment.

Studying Fig. 4.7(top right), we indeed see that the modified inverse participation ratios are bigger than the inverse participation ratios. For example, for $\mathcal{M} = 0.4$, the inverse participation ratio at $S = 0.4$ has an average value of 21, whereas the modified participation ratio at $S = 0.4$ is 38. Moreover, on average the inverse participation ratios for a modularity of 0.4 reach 64 by $S = 0.84$, whereas the average modular inverse participation ratios reach 64 far more quickly: at $S = 0.58$. Comparing Fig. 4.7(bottom left) and Fig. 4.7(bottom right), we see that similar results hold for comparisons of the modular participation and modified

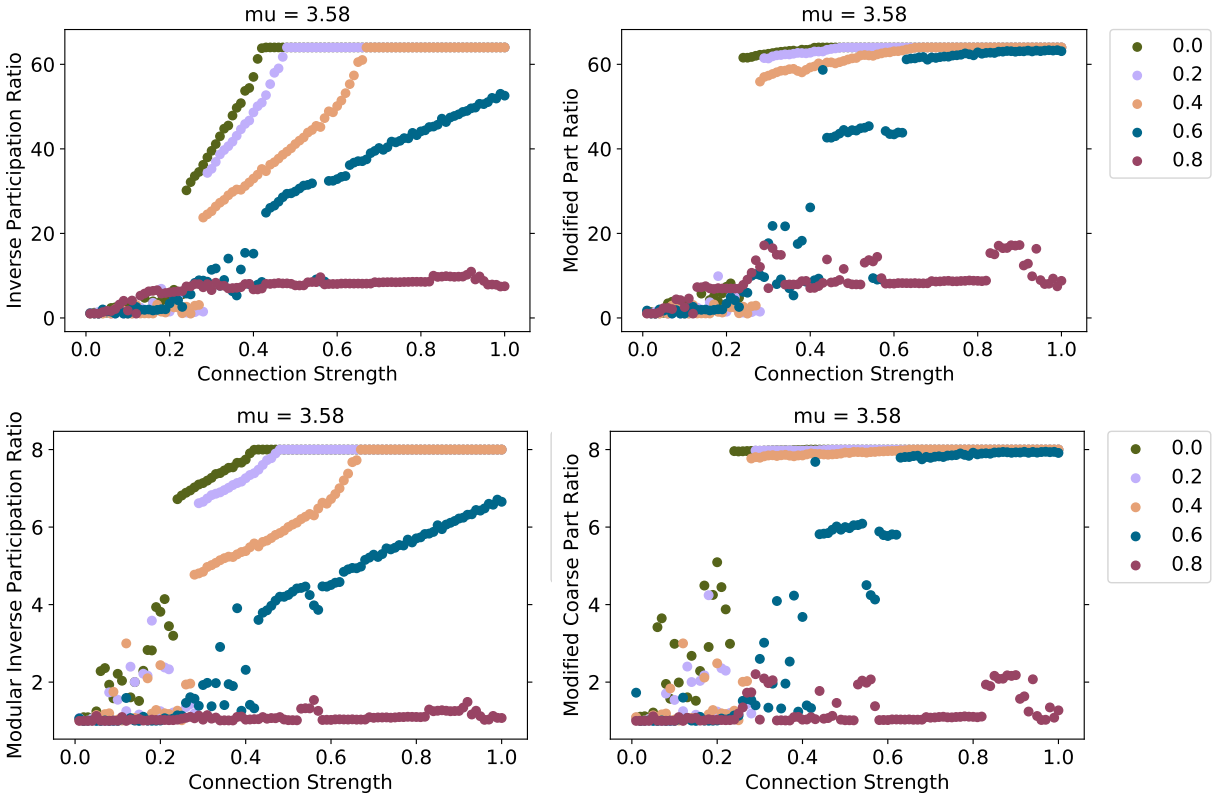

Figure 4.9: Top Left: Inverse participation ratios of individual networks for $k = 4, M = 8, N = 8$. Bottom Left: Modular inverse participation ratios. Top Right and Bottom Right: The modified inverse participation ratio and coarse participation ratios, respectively. Legend: Modularity runs from 0 to 0.8.

modular participation ratios. These differences indicate that the perturbations are spreading on average between the different modules and nodes over time. However, we see that this is only true for the transition region, roughly $0.25 < S < 0.85$, since the networks are behaving globally (i.e. the whole system is contributing to the perturbation because it is highly connected) in the regions above the transition region and locally (i.e. perturbations are centered entirely on one node or module) for regions below the transition region.

Comparing the behavior of the inverse participation ratio to our modified in-

verse participation ratio for individual networks yields even more insight about the behavior as a function of S. In Fig. 4.9(top right) and Fig. 4.9(bottom right), for $\mathcal{M} \lesssim 0.5$, we see an extremely abrupt jump in the modified participation value from a small value to a value very close to the maximum allowed. For an individual network, the transition appears to be truly local to global. Comparing those to the panels directly to their left (the "traditional" inverse participation ratios), we see that the jump is more extreme in the modified version. The difference in the graphs between $0.2 \lesssim S \lesssim 0.35$ is because the perturbation does not involve all nodes at any given moment, involving different nodes over time until it spends time on all nodes — the perturbation spreads globally, but not all at once.

Modularity of 0.8

Now that we know the behavior of the participation ratios, we can analyze the modularity of 0.8 case in more detail. From Fig. 4.1, we know that the Lyapunov exponent of the modularity 0.8 case is much different than the other modularities; instead of a minimum and then a slow rise back to the maximum as connection strength increases, the modularity 0.8 ensemble has a steep incline around $S = 0.15$, followed by a slow decline starting at $S = 0.2$. The key to understanding this decline is to note that the inverse participation ratios, as seen in Fig. 4.7, are around 8 for this range, indicating that the perturbation lies in one module. Running simulations of the populations of each node reveals the modules are synchronized;

all nodes in each module have the same population value. Now, we posit that for a modularity of 0.8, the slow decrease in λ_1 from $S = 0.2$ to 1.0 is similar to the initial decrease in Lyapunov exponents explained in Sect. 4.1, but this time the modules are acting as single nodes, and a greater amount of sharing makes the $\mu_{effective}$ decrease (but only slightly – not enough to reach stability).

We can rearrange Eq. (3.4) to express what happens to a node in a network with high modularity; in such a network, $k-1$ connections are in the same module, which are synchronized, and one node is outside the module. To show this, we describe what happens to an effective μ in a network with these qualities:

$$f(x_i) = (1-S)\mu x_i(1-x_i) + \frac{S}{k}\sum_{j}^{k} \mu x_j(1-x_j)$$

where x_i is the node population in question and x_j are the node populations of the connected nodes. Then, since on average, $k-1$ nodes are in the module (meaning they are synced) and 1 node is outside the module (meaning it is not synced), we can transform the sum in the following way:

$$f(x_i) = (1-S+\frac{k-1}{k}S)\mu x_i(1-x_i) + \frac{S}{k}\mu x_j(1-x_j)$$

where there are $k-1$ nodes all with the same population, which is where the first term arises. This gives

$$f(x_i) = (1 - \frac{1}{k}S)\mu x_i(1 - x_i) + \frac{S}{k}\mu x_j(1 - x_j).$$

So we get a new $\mu_{effective}$ where

$$(1 - \frac{S}{k})\mu < \mu_{effective} < \mu \tag{4.2}$$

So by increasing S, we see a decline in the chaos because $\mu_{effective}$ decreases. This decrease is much later than that in Eq. (4.1) because of the factor of $1/k$ in front of S of Eq. (4.2). This is similar to renormalization in statistical physics, where our "block spins" are the modules and the effective μ is changed.

4.3 Percent of Contribution in Largest Module

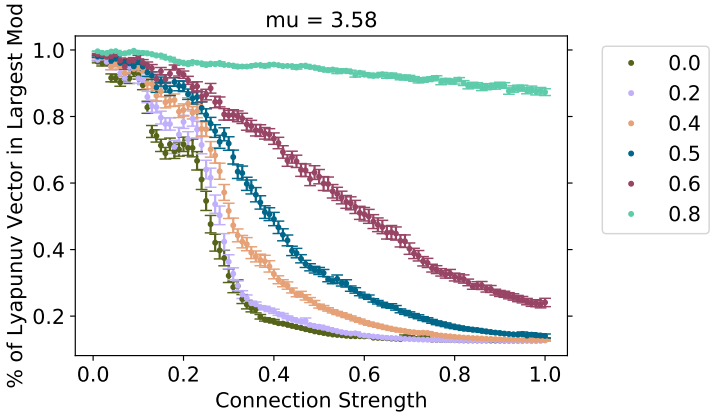

Figure 4.10: Percent of Contribution in Largest Module, for $k = 4, M = 8, N = 8$.

Another way to measure how broadly the perturbations spread is to calculate what fraction of the Lyapunov vector is contained in each node and report

the maximum value. In networks where the instabilities are highly-localized, this value should be large, indicating the involvement of mostly just one module. In networks where the instability is global, this number should approach $1/8 = 0.125$, since there are 8 modules. The results of such calculations are shown in Fig. 4.10. The percent of contribution in the largest module gives further evidence that perturbations in networks of higher modularity (0.8 modularity) do not escape from a module. For smaller modularities, we also see evidence of the nodes transitioning from local to global behavior: if the percent of the Lyapunov vector in the module with the highest percent of Lyapunov contributions is 0.125 (or 1/8), this means each of the other modules also contribute to one eighth of the vector. The figure aligns with our intuition that as modularity increases, the perturbation belongs more wholly to one module.

4.4 Non-Chaotic values of μ

Since networks of chaotic elements can become non-chaotic under certain conditions, we decided to test whether the opposite would also be true — whether networks of non-chaotic elements would become chaotic under certain conditions. We ran a variety of tests on networks with $\mu = 3.569$, which is just below the value of μ where the logistic map changes from periodic to chaotic behavior. For the same connectivity $k = 4$ as above, and 64 nodes spread into 8 moodules, as above, we found that the Lyapunov exponents for all modularities indicated stability.

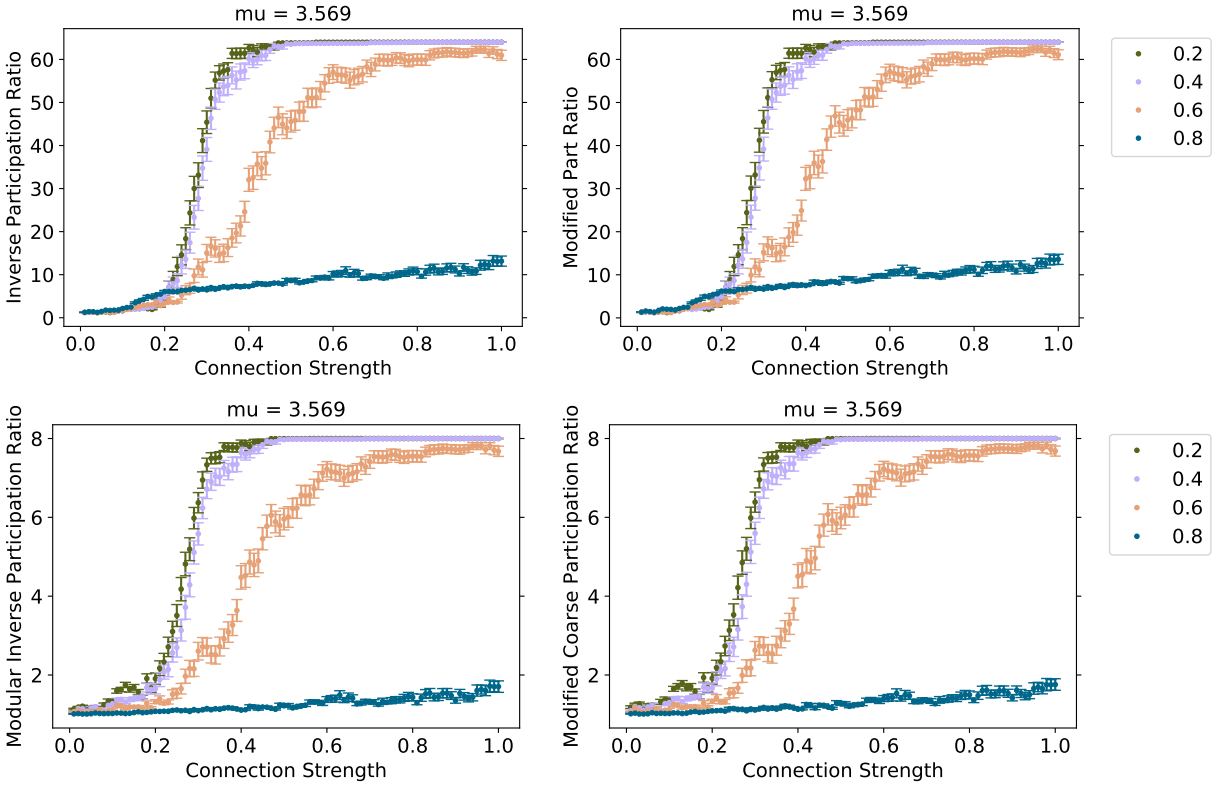

Figure 4.11: Plots of inverse participation ratio, coarse inverse participation ratio, modified participation ratio, and modified coarse (modular) participation ratio. Modularity is varied, and the other parameters are kept at the defaults ($k = 4, M = 8, N = 8$.) Notice that the inverse participation ratios behave the same as their modified versions.

It is also interesting to note that the periodic behavior does not change the general schema of the inverse participation ratios. In Fig. 4.11, we see very similar behavior of the inverse participation ratios to the chaotic case in Fig. 4.7. The surprising part is that the nodes transition more quickly from local to global behavior.

An interesting facet of figure 4.11 is that the modified participation ratio and the modified coarse participation ratios are indistinguishable from the non-modified versions. This suggests that the perturbations, when located in one module or on a set of nodes, stay in the same module or are located on the same nodes.

4.5 Degree of Connectivity and Stability

There are several other parameters in our networks that can be varied. We have not performed exhaustive explorations of these, but we have done some preliminary studies. For networks of 64 nodes divided into 8 modules and $\mu = 3.58$, we studied how exponents and participation ratios varied with the number of connections per node k. As can be seen in Fig. 4.12, after $S \approx 0.35$ perturbations distribute evenly on nodes for most degrees of connectivity, as shown by the large values of the inverse participation ratios. We also observe that after $S = 0.20$, the higher the degree of connectivity, the higher the first Lyapunov exponent. More nodes are connected to each other, which makes the transition between a local state and a global state sharper and thus makes the system more chaotic. However, for

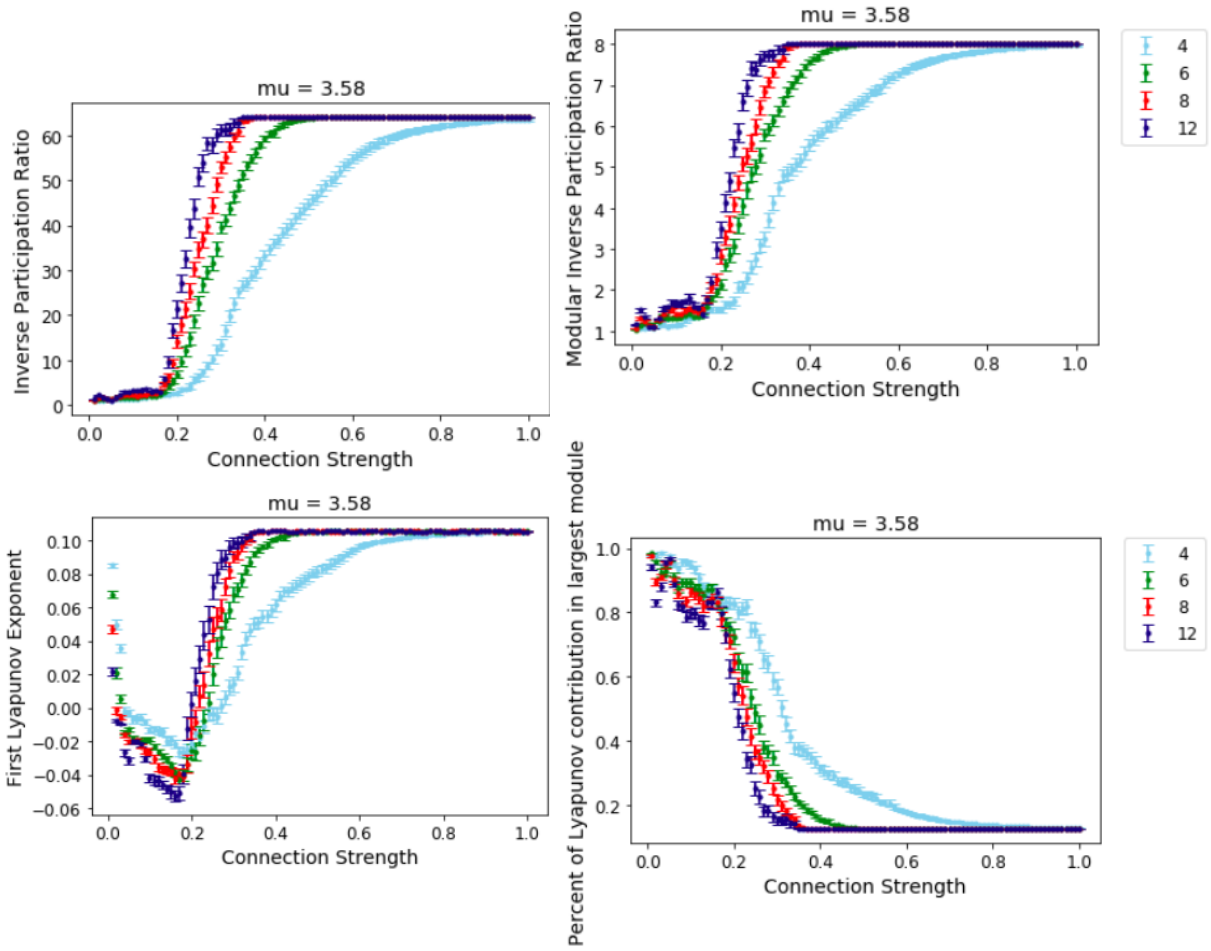

Figure 4.12: Plots of inverse participation ratio, coarse inverse participation ratio, first Lyapunov exponent, and percent of largest Lyapunov contribution in largest module. Degree of connectivity is varied, and the other parameters are kept at the defaults ($P = 0.5, M = 8, N = 8.$) Before $S = 0.2$, the exponents support the claim that higher k values are less stable, whereas after $S = 0.2$, they contradict this claim.

$S \leq 0.20$, higher degrees of connectivity correspond to more stable behavior (where more stable means more negative first Lyapunov exponent). This is the opposite of what Gardner and Ashby [3] and May [4] found, but both groups worked with non-chaotic elements, so this does not directly contradict their conclusions. Further research is needed on the negative exponents which arise for small connection strength values.

In Fig. 4.13, we show how the inverse participation ratio, the modular inverse participation ratio, and λ_1 vary with S for 4 different modularities, each for $k = 4$ and $k = 8$. Most of the data follows the observations from the previous graph with the higher k value showing larger numbers of participating nodes and modules for the same S. The most interesting difference is in the Lyapunov exponent for the highest modularity system. For $k = 4$, networks are unstable for almost all values of S; however, for $k = 8$, there is a broad plateau of stable values between $S \approx 0.05$ and $S \approx 0.5$.

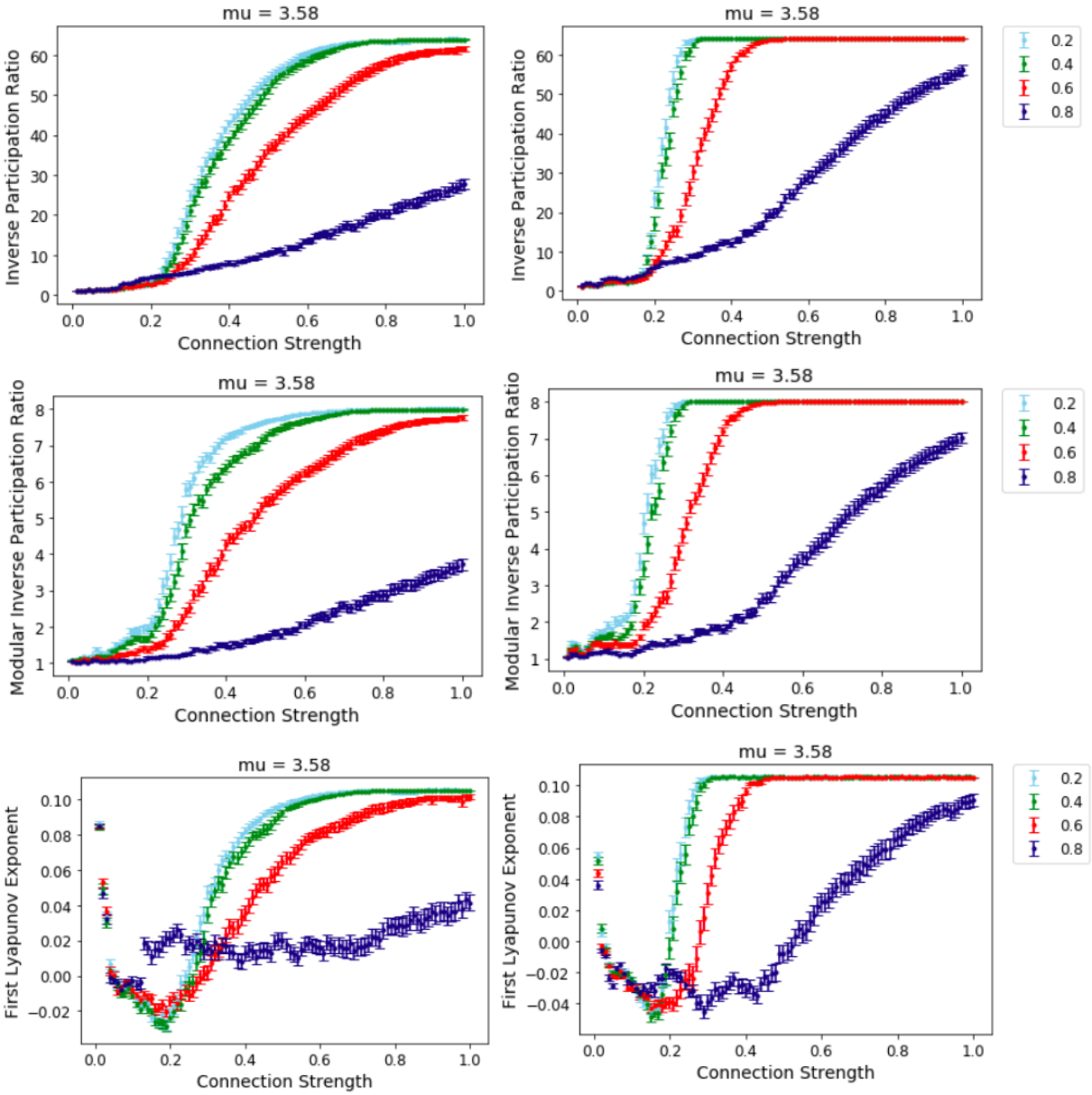

Figure 4.13: Measures of inverse participation ratios, coarse inverse participation ratios, and first Lyapunov exponents for $M = 8, N = 8$. Left column: $k = 4$. Right column: $k = 8$. Again, the Lyapunov exponents broadly support the claim that higher degree of connectivity means less stability, except for the region between $S = 0.01$ and $S = 0.20$.

4.6 Network Size and Stability

Gardner and Ashby [3] and May [4] found that larger networks were more likely to be unstable than smaller ones. For modular systems, there are two ways to make the network larger — increase the number of modules or increase the number of nodes per module.

Fig. 4.14 shows the results of simulations on networks with varying numbers of modules, but with the number of nodes per module fixed. For more modules in a system, we see that our results agree with Gardner and Ashby [3] and May [4] for $S \lesssim 0.25$ (more modules is less stable); however, for $S \gtrsim 0.25$, we see the opposite effect — increasing the number of modules makes the networks less unstable.

Fig. 4.15 shows the results of simulations on networks with varying numbers of nodes per module, but with the number of modules fixed. In this case, we find a similar result – that our results agree with Gardner and Ashby [3] and May [4] for $S \lesssim 0.25$ (more modules is less stable); however, for $S \gtrsim 0.25$, we see the opposite effect — increasing the number of nodes per module makes the networks slightly less unstable.

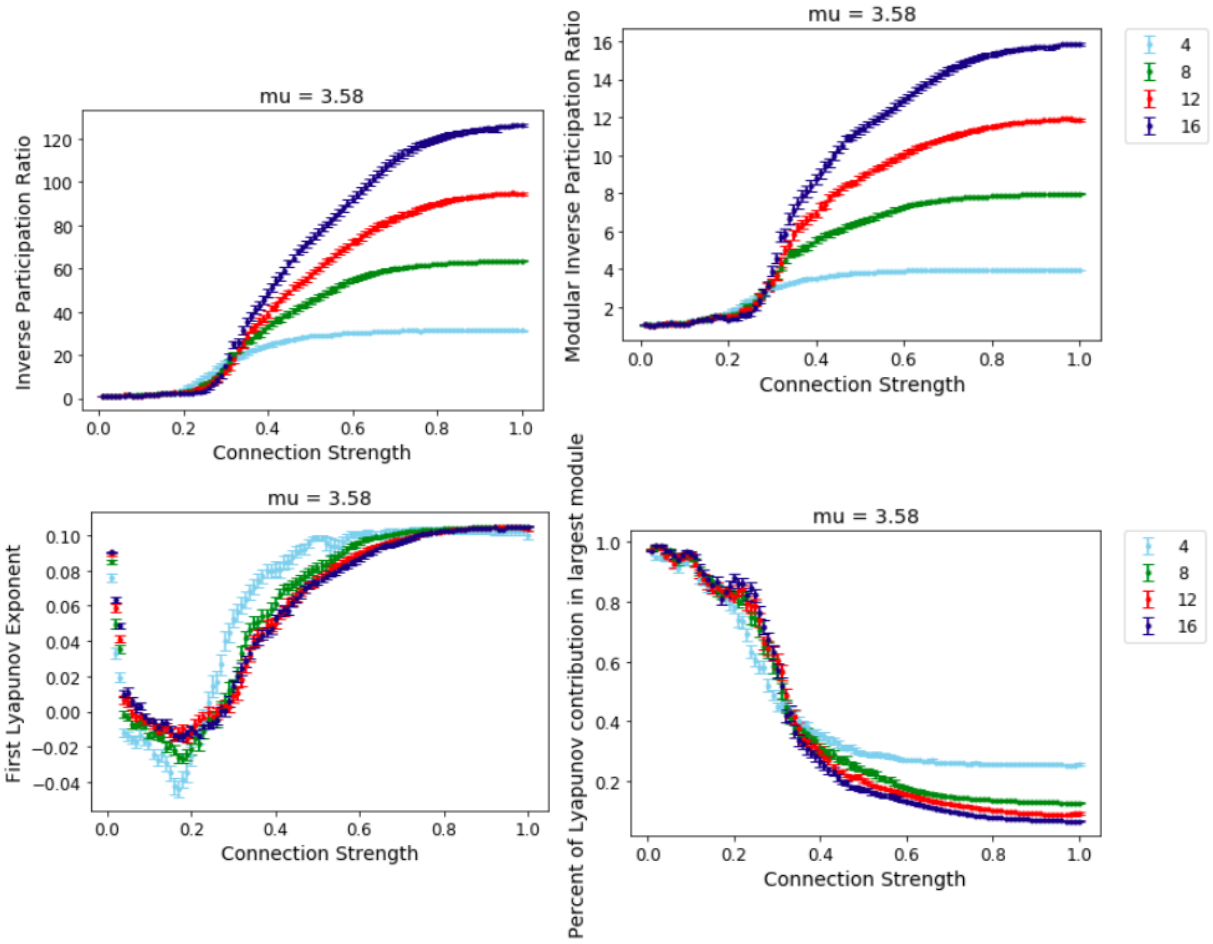

Figure 4.14: Measures of inverse participation ratios, coarse inverse participation ratios, and first Lyapunov exponents for $P = 0.5, k = 4, N = 8$, where M (number of modules) is varied. The Lyapunov exponent graph for $S > 0.25$ broadly contradicts the claim that more modules mean less stable (more chaotic) behavior.

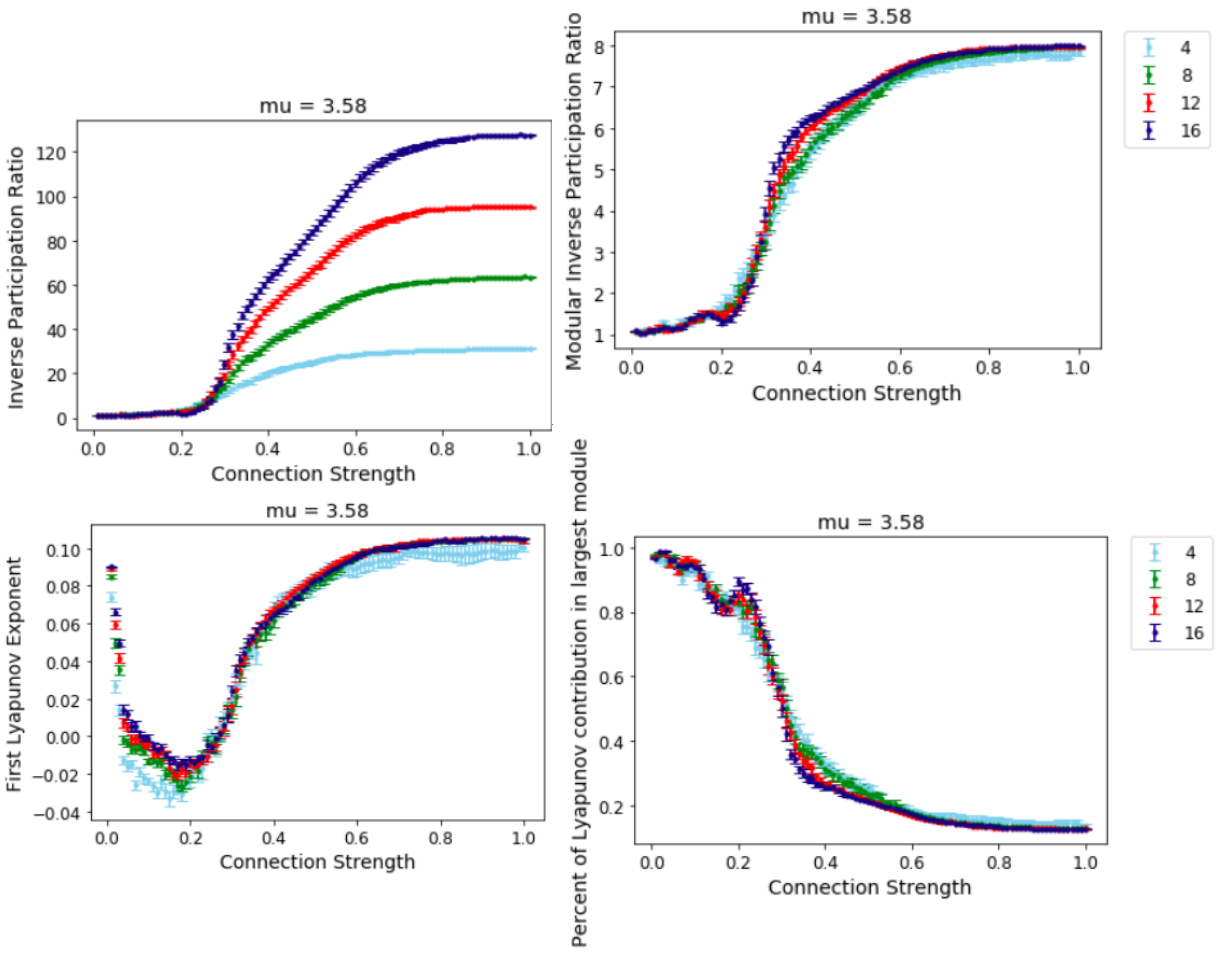

Figure 4.15: Measures of inverse participation ratios, coarse inverse participation ratios, and first Lyapunov exponents for $P = 0.5, k = 4, M = 8$, where N (number of nodes per module) is varied. The Lyapunov exponent graph for $S > 0.25$ somewhat contradicts the claim that more nodes per module mean less stable (more chaotic) behavior.

Chapter 5

Conclusions and Future Work

We have explored the dynamical behaviors of networks of chaotic elements under various conditions, with a particular focus on the spread of perturbations and the effect of modularity. In contrast to the earlier work of Gardner and Ashby [3] and May [4], we found very few simple relationships between stability and network properties such as connection strength, connectivity, network size and modularity. Although our work is on-going, we have reached a number of conclusions.

For low to moderate modularity systems, surprisingly, we found a range of connection strengths that led to stable networks (negative Lyapunov exponents). Somehow sharing a small amount of information (population) with neighbors removed the chaotic dynamics. Interestingly, the Lyapunov vectors were localized to a few nodes, indicating that this stabilization was a local effect (but occurring everywhere).

For slightly higher values of the connection strength (again for low to moderate modularity) we discovered a discontinuous transition from the stable, localized dynamics to a global, chaotic dynamics with a spread of the perturbations to all nodes. This transition occurs at a different value of S for individual networks. The initial discontinuous transition is from one or two nodes to a chaotic perturbation mode that does not span all (usually 64) nodes at any moment, but that visits (leaks to) all nodes over time. For even stronger connection strengths, the behavior eventually becomes globally synchronized chaos.

For the largest modularities we studied, we found that the system is unstable for almost all connection strengths, but the spread of instabilities was indeed contained approximately within one module at all times. Interestingly, the strength of the chaotic fluctuations decreased as the connection strength was increased for most of the parameter range. In addition, the highly modular networks were usually more chaotic than less modular ones.

We have also performed preliminary tests of varying network connectivity (average degree of each node) and network size. In these tests, we found a transition between behaviors at around a connection strength of $S = 0.20$. Below this value the relationship between stability and the parameter (connectivity, for example) would go in one direction, but above the value, the relationship would go in the other direction.

We also tested a network of non-chaotic logistic maps ($\mu < 3.569946...$) and

found that the networks were always stable; however, these networks still exhibited inverse participation ratio graphs that were quite similar to the chaotic ones, including a transition from local to global dynamics.

Obviously, there is a great deal more that we can study in this fascinating system. However, two main tasks stand out as most important to explore next. The first is how a network of chaotic elements can be stabilized by a small amount of coupling, especially since the phenomenon appears to be local. The second is to understand how networks transition from local dynamics to global dynamics, and what network properties determine the transition point.

A further exciting direction would be to test how our results change if we modify the dynamical process on the nodes, perhaps to models relevant to disease propagation in the middle of a pandemic...

Chapter 6

Appendix

6.1 Lyapunov dimension

The Lyapunov dimension is computed by summing exponents starting from the largest (first) exponent and ending when the sum drops below zero [26]. The dimension is the number of exponents at which the sum becomes zero. In a stable system (where all the exponents are negative) the Lyapunov dimension is always zero. If the sum of all N exponents is positive, then the dimension is N.

We do not always have an integer dimension; we use interpolation to determine the point where the sum turns from positive to negative. For example, if we have Lyapunov exponents of 6, 3, -1, -4, -5, -8, and -9, the sum is 4 after the fourth exponent and -1 after the fifth exponent — hence the Lyapunov dimension is $4 + 4/(4+1) = 4.8$.

The Lyapunov dimension can roughly be thought of as the number of orthogonal perturbation modes with large enough growth rates to affect the dynamics of the network — the number of mostly dynamically-independent collections of nodes. Lyapunov vectors with positive or slightly negative exponents persist long enough to significantly affect the population of the network, whereas vectors with strongly negative exponents disappear quickly and do not have much effect on the system.

References

[1] D. Helbring. Globally networked risks and how to respond. *Nature*, 497:51–59, 2013.

[2] P. Holme, B.J. Kim, C.N. Yoon, and S.K. Han. Attack vulnerability of complex networks. *Phys. Rev. E*, 65:056109, 2002.

[3] M.R. Gardner and W.R. Ashby. Connectance of large dynamic (cybernetic) systems: Critical values for stability. *Nature*, 228:784, 1970.

[4] R.M. May. Will a large complex system be stable? *Nature*, 238:413–414, 1972.

[5] Ben Stein-Lubrano. Modularity, stability, and chaotic dynamics in networks. 2019.

[6] R.H. MacArthur. Fluctuations of animal populations and a measure of community stability. *Ecology*, 36:533–536, 1955.

[7] C.S. Elton. *The Ecology of Invasions by Animals and Plants*. Chapman & Hall, London, 1958.

[8] K.E.F. Watt. *Principles of Environmental Science*. McGraw-Hill, New York, 1973.

[9] M.A. Fortuna, A.G. Popa-Lisseanu, C. Ibáñez, and J. Bascompte. The roosting spatial network of a bird-predator bat. *Ecology*, 90:934–944, 2009.

[10] Luis J. Gilarranz, Bronwyn Rayfield, Gustavo Liñán Cembrano, Jordi Bascompte, and Andrew Gonzalez. Effects of network modularity on the spread of perturbation impact in experimental metapopulations. *Science*, 357:199–201, 2017.

[11] M.T. Fountain and S.P. Hopkin. Folsomia candida (collembola): A "standard" soil arthropod. *Annu. Rev. Entomol.*, 50:201–222, 2005.

[12] J.R. Beddington. Age distribution and the stability of simple discrete time population models. *J. Theor. Biol.*, 47:65–74, 1974.

[13] P. Erdös and A. Rényi. On the evolution of random graphs. *Publ. Math. Inst. Hungar. Acad. Sci.*, 5:17–61, 1960.

[14] M.E.J. Newman and M. Girvan. Finding and evaluating community structure in networks. *Phys. Rev. E*, 69:026113, 2004.

[15] Roger Guimerà and Luís A. Nunes Amaral. Functional cartography of complex metabolic networks. *Nature*, 433:895–900, 2005.

[16] P. Grassberger and I. Procaccia. Measuring the strangeness of strange attractors. *Physica*, D9:189–208, 1983.

[17] P. Manneville. *Liapounov exponents for the Kuramoto-Sivashinksy model*, volume 230 of *Lecture Notes in Physics*, pages 319–326. Springer-Verlag, 1985.

[18] Kunihiko Kaneko. Lyapunov analysis and information flow in coupled map lattices. *Physica D*, 23:436–447, 1986.

[19] S. Ciliberto. Fractal dimension and metric entropy in extended systems. *Europhys. Lett.*, 4(6):685–690, 1987.

[20] H. Chaté. Lyapunov analysis of spatiotemporal intermittency. *Europhys. Lett.*, 21(4):419–425, 1993.

[21] D.A. Egolf and H.S. Greenside. Relation between fractal dimension and spatial correlation length for extensive chaos. *Nature*, 369:129–131, 1994.

[22] D. A. Egolf. Dynamical dimension of defects in spatiotemporal chaos. *Phys. Rev. Lett.*, 81:4120–4123, 1998.

[23] D.A. Egolf, I.V. Melnikov, W. Pesch, and R.E. Ecke. Mechanisms of extensive spatiotemporal chaos in Rayleigh-Bénard convection. *Nature*, 404:733–736, 2000.

[24] M.P. Fishman and D.A. Egolf. Revealing the building blocks of spatiotemporal chaos: Deviations from extensivity. *Phys. Rev. Lett.*, 96:054103, 2006.

[25] E.J. Banigan, M.K. Illich, D.J. Stace-Naughton, and D.A. Egolf. The chaotic dynamics of jamming. *Nat. Phys.*, 9:288–292, 2013.

[26] E. Ott. *Chaos in Dynamical Systems*. Cambridge University Press, Cambridge, 1993.

[27] J. H. Greene and J. Kim. The calculation of Lyapunov spectra. *Physica*, 24D:213–225, 1987.